

# Silicon thermal flow sensors

B W van Oudheusden

*Electronic Instrumentation Laboratory, Department of Electrical Engineering, Delft University of Technology,  
P O Box 5031, 2600 GA Delft (Netherlands)*

## Abstract

This paper discusses the design and application of silicon thermal flow sensors. It is shown how the transduction path in the complete measurement system, going from flow variable to electrical signal, results in three fundamental problems, which can be associated with, respectively, the mechanical, thermal and electrical signal domains. These aspects are further discussed in relation to the silicon flow-sensor research performed at the Electronic Instrumentation Laboratory.

## 1. Introduction

Among the fields of interest for the application of silicon sensors, certainly one of great interest and challenge is that of fluid flow (denoting both liquid and gas flow). Man has always been intrigued by flow phenomena, and in many cultures flow has become the very symbol of elusiveness and unpredictability, whereas also in more recent times much effort has been devoted to the understanding of fluid flow. Apart from this rather scientific interest, flow phenomena have a direct practical significance in many industrial, technical and everyday situations in meteorology (wind velocity and direction), civil engineering (wind forces on buildings and constructions), transport and process industry (fluidic transport of media, combustion, vehicle performance), environmental sciences (dispersion of pollution), biomedics (respiration and blood flow), and indoor climate control (ventilation), to mention but a few. Two very typical examples of the many possible flow-measurement problems are

(a) Flow velocity measurement: the flow velocity is a vectorial quantity which describes the local situation in a flow field. When the direction of the flow is known, a measurement of the magnitude of the flow is sufficient. In other cases a directionally sensitive measurement may be required to determine the different velocity components.

(b) Fluidic transport rate: in the case where the flow is confined to a restricted space (pipe or

channel) the total amount of fluid (mass or volume) passing through it per unit of time is to be determined.

### 1.1 Flow measurement techniques

The physical basis on which most flow-sensing techniques rely is either the momentum of the flowing medium or its transporting ability. The former principle is the basis on which mechanical transducers operate, like those employing the direct detection of the pressure or force which the instrument experiences as a result of the flow (pressure tubes, for example). Alternatively, a kinematic method can be used, where a part of the instrument is set in rotary motion by the flow, the rate of rotation being linearly proportional to the flow velocity (rotating-cup and propeller anemometers). The implementation of the transport principle comprises the tracing of a detectable agent which is carried along by the flow, using, e.g., heat, smoke, dust particles or a radioactive contaminant.

Thermal flow sensing relies on the thermal interaction between sensor and flow [1]. According to the underlying physical principle, the following sensing techniques can be distinguished.

*The cooling of a hot object:* the heat which is transferred from a heated element in a fluid stream depends (non-linearly) on the flow velocity.

*Heat transport:* mass flow can be measured as heat transport by determining the heat content of the fluid that passes.

*Thermal tracing* the transport of heat in a flow can be traced by timing the passage of a heat pulse over a known distance (time-of-flight measurement)

### 1.2 Silicon flow sensors

Flow can be measured with a silicon sensor if there is a physical effect present to provide the interaction between the flow and the electrical behaviour of the components of the sensor IC [2]. A limited number of silicon flow sensors that operate on a mechanical transduction principle (pressure or force measurements) have been reported in the literature [3–6]. Thermal principles have proved to be especially attractive for application in silicon flow-velocity and mass-flow sensors, because of their structural and electronic simplicity. As no additional non-electronic components are required, complete integration in standard silicon technology is possible. No (or only very few) modified or additional processing steps are required, which is desirable as this would otherwise limit the possibilities of producing the sensor and increase its cost. In addition, the sensor can be shielded by a thermally conducting cover layer so that direct contact between the sensor and the fluid can be avoided. The sensor operation is based either on the heat transfer from the sensor, or on the measurement of a flow-induced temperature gradient. This second principle has been used in the Electronic Instrumentation Laboratory for the development of a class of integrated flow sensors, including both bi- and omnidirectional variants, the latter having a full 360° sensitivity [7].

#### 1.3 Design aspects of thermal-flow sensors

To discuss the various aspects involved in the design and use of a complete flow-measurement system, let the configuration of Fig. 1 be considered. It represents a flow sensor probe, which comprises a thermal sensor and operates on the principle of flow-induced temperature differences. The non-uniform heat transfer from the sensor to the flow over the sensor probe results in a temperature difference in the sensor. The signal transduction path is illustrated by the block diagram in the Figure. A number of subsequent basic transduction steps can be distinguished in the sensor operation, going from the mechanical via the thermal to the electrical signal domain. Accordingly, different

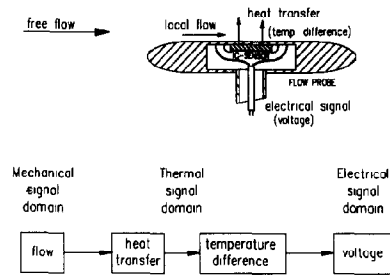


Fig. 1 Signal transduction in a generic thermal flow sensor (probe shown in cross section)

aspects of, respectively, mechanical, thermal and electronic nature can be distinguished.

The mechanical aspect is associated with the relation between the flow parameter to be measured (like the wind force, or the total flow rate through a pipe) and the local flow that exists in the immediate vicinity of the sensor and which determines its operation. This is particularly relevant in any application, and important topics in this respect are the mounting of the sensor device and the design of probe shapes and flow channels.

The thermal aspect deals with the interaction of the local flow and the sensor through heat-transfer effects, and is also concerned with the different sensor operation modes which can be applied (e.g., temperature, temperature-gradient or power measurement) and the analysis of thermal effects that may interfere with or limit the sensing operation (temperature control and compensation).

The electronic aspect concerns, first of all, the accurate, sensitive and reliable generation of an electrical measurement signal representing the flow-induced thermal effect, and further, the processing of the measurement signals. In the case of integrated sensors and smart instrumentation systems, this second function may be partially combined with the sensing operation or performed on the sensor device itself.

With these transduction steps through the different physical signal domains, three major transduction problems in the design of a flow sensor for a specific application have to be dealt with, namely the flow problem, the thermal problem and the electronic problem. Each of these problems pertains to a separate discipline, and this illustrates how the development of sensor research is inherently a multidisciplinary activity. In the case of a silicon thermal-flow sensor we have, in general, to

deal with fluid dynamics, thermodynamics, semiconductor physics and electronics. These various aspects are discussed further in Section 2. The emphasis lies on thermal sensor mechanisms, and their possibilities for implementation. This is the central problem, which sets the conditions for the two other problems. For the flow problem, it reveals which aspect of the flow determines the sensor response. For the electronic problem, it dictates which thermal parameters have to be measured.

## 2. Silicon thermal anemometers

The heat loss from a hot sensing element immersed in a fluid increases with the flow rate. Sensors employing the relation between the heat transfer and the flow are usually referred to as thermal anemometers (derived from the Greek word *anemos*, meaning wind). They have been widely used since the introduction of the hot-wire anemometer at the beginning of this century.

### 2.1 Theoretical principle of operation

In addition to the heat carried away by the flow,  $Q_f$ , heat is conducted to the carrier substrate to which the sensor is mounted,  $Q_c$ . To obtain a steady-state situation, the heat transfer must be balanced by the power dissipation  $P$  in the sensor.

$$P = Q_c + Q_f = G_c(T_s - T_{\text{sub}}) + G_f(T_s - T_f) \quad (1)$$

where  $T_s$ ,  $T_{\text{sub}}$  and  $T_f$  are the temperature of the sensor, its substrate and the fluid at a large distance from the sensor, respectively. When a good thermal coupling exists,  $T_{\text{sub}}$  and  $T_f$  can be taken as equal to the ambient temperature.  $G_c$  and  $G_f$  stand for thermal conductances (that is, the heat transfer per unit temperature difference) due to conduction and convection, respectively. Other flow-independent heat-transfer effects, like radiation, can be included in  $G_c$ . The flow measurement relies on the dependence of  $G_f$  on the flow, and this relation is now discussed for some simple cases.

#### Calorimetric principle

A thermal mass-flow meter can be constructed by directly measuring the heat content of the passing fluid in a closed channel. A first sensor measures the temperatures  $T_f$  of the unaffected,

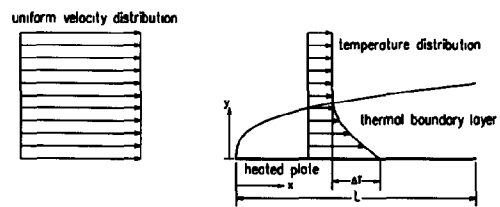
incoming fluid, and another that of the heated, outgoing fluid, which is assumed equal to that of the sensor,  $T_s$ . The amount of heat  $Q_f$  which is supplied to the fluid is proportional to the temperature rise of the fluid.

$$Q_f = c_p \phi_m (T_s - T_f) \quad (2)$$

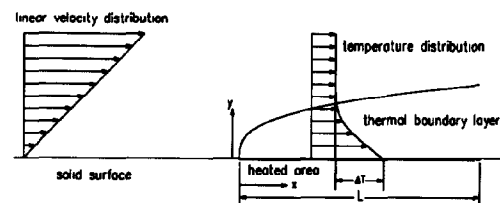
where  $c_p$  is the specific heat of the fluid and  $\phi_m$  the mass flow (in kg/s). Comparison with eqn (1) shows that, hence,  $G_f = c_p \phi_m$ . The assumption that the complete flow that passes is heated (total heating) is essential here, because only in that case is the heat content of the entire flow measured correctly.

#### Boundary layer principle

Above a certain flow speed in a pipe, or when the sensor is not in a restricted space, only a region of the flow near the sensor is heated, and a thermal boundary layer is formed over the sensor. As the thickness of the boundary layer (and therefore the amount of flow that is affected) decreases with increasing velocity, the heat transfer increases less than linearly in relation to the flow speed. For the two simple geometries illustrated in Fig. 2, an analytic solution can be formulated in the case of laminar flow [8]. The first case is that of a heated thin plate placed parallel to a flow of uniform velocity  $U$  (flat plate flow). When the plate has a



(a)



(b)

Fig. 2 Heat transfer in thermal boundary layers (a) flat plate flow, (b) uniform shear flow

constant temperature  $\Delta T$  above that of the flow, the surface heat flux per unit area,  $q_f$ , for one side is given by

$$q_f = 0.332 k_f \Delta T Pr^{1/3} \left( \frac{U}{xv} \right)^{1/2} \quad (3)$$

where  $x$  is measured from the upstream edge of the plate,  $k_f$  and  $\nu$  are the conductivity and kinematic viscosity of the fluid and  $Pr$  the Prandtl number

The second configuration is that of a linear flow profile ( $dU/dy = \text{constant}$ ) over a surface element of uniform temperature, where we find the expression

$$q_f = 0.538 k_f \Delta T Pr^{1/3} \left( \frac{dU/dy}{xv} \right)^{1/3} \quad (4)$$

where  $x$  is now measured from the upstream edge of the heated region and  $y$  normal to the surface. For the laminar flow of a Newtonian fluid, the shear stress  $\tau$  is proportional to the velocity gradient  $dU/dy$ , and so in this case is constant throughout the flow field. For this reason this type of flow is also referred to as constant, or uniform, shear flow.

The value of the thermal conductance  $G_f$  is obtained by integrating  $q_f$  over the entire surface  $A = WL$  (where  $W$  and  $L$  denote the width and length of the heated surface), and dividing by  $\Delta T$ . Hence, we find for laminar flow that  $G_f$  increases in proportion to  $U^{1/2}$  and  $\tau^{1/3}$ , respectively. Note that we can write the expression for the local heat transfer  $q_f$  as a product of its average value  $G_f \Delta T/A$  and a distribution function

$$q_f = \frac{G_f \Delta T (x/L)^{-n}}{A (1-n)} \quad (5)$$

with  $n = 1/2$  for flat plate flow and  $n = 1/3$  for shear flow.

For a realistic configuration like that of the flow probe illustrated in Fig 1, the analysis is much more complex. However, a similar dimensional relation between  $G_f$  and the upstream velocity  $U$  or the local value of the surface shear stress  $\tau$ , is obtained. As for laminar flow  $\tau$  varies in proportion to  $U^{3/2}$ , the two expressions in that case yield corresponding results for the velocity calibration, namely that  $G_f$  increases with  $U^{1/2}$ .

## 2.2 Practical operation of thermal anemometers

For a particular sensor the relation between the power dissipation  $P$  at steady state, the flow velocity

$U$  and the temperature elevation of the sensor  $\Delta T = T_s - T_{\text{amb}}$  can be written as

$$\frac{P}{\Delta T} = G_0 + KU^{1/2} \quad (6)$$

where  $G_0$ , the zero-flow conductance, and  $K$ , the flow sensitivity, are parameters which for simple sensor geometries can be estimated from theoretical analysis. However, as it is hardly possible to include in the analysis all relevant effects with sufficient accuracy, additional experimental calibration of a sensor is usually indispensable.

### Operation modes

A thermal-flow sensor can be operated in different ways, of which the most important are those where either the total power dissipation or the sensor temperature is maintained at a constant value (see Fig 3). When using constant power dissipation, the temperature of the sensor decreases with the flow velocity, and this variation determines the flow measurement. In practice, a simpler approach is often followed by maintaining only the supply voltage or current constant, and applying a correction for the variation in power dissipation. Constant power operation has the advantage that its electronic implementation is very simple, but an unfavourable aspect of it is that, due to the variation of the sensor temperature, the temperature sensitivity of the sensor and fluid properties must be taken into account. Also, the response speed of the sensor is limited by its thermal capacity; the time constant is equal to  $C/G$ , where  $C$  is the thermal capacity of the sensor and  $G$  the total thermal conductance. This can be improved to a great extent by operating the sensor at a constant temperature, which is achieved by applying a feedback amplification loop in the circuit controlling

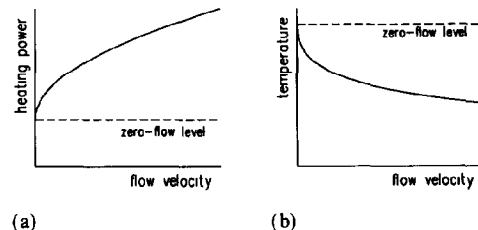


Fig 3 Thermal anemometers (a) constant-temperature operation, (b) constant-power operation

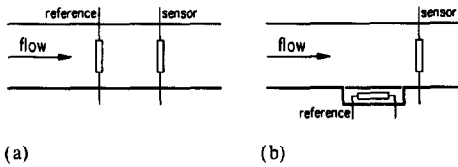


Fig 4 Thermal anemometers (a) temperature reference method, (b) zero-flow reference method

the heating of the sensor. Alternatively, the temperature difference between sensor and flow can be maintained constant, rather than the absolute sensor temperature, to correct for variations in the ambient temperature.

The power dissipation  $P$  and the sensor temperature  $T_s$  are quantities that can be obtained directly from the sensor operation. However, as can be seen from eqn (6), the absolute sensor temperature is not relevant for the flow measurement, but rather the temperature difference between the sensor and the flow. A reference measurement or reference sensor is therefore required to be able to determine the flow velocity completely.

In the practical implementation two different methods can be distinguished: the temperature reference and the zero-flow reference methods (Fig 4). In the temperature reference method, the fluid temperature is explicitly measured using a reference sensor in which the power dissipation is so small that the effect of self-heating is negligible, hence that sensor adopts the temperature of the flow. The measured flow temperature can then be used to calculate the temperature difference between the sensor and the flow, or it can be employed to regulate this temperature elevation at a constant level. In the zero-flow reference method two equal sensors are operated under identical conditions (equal power dissipation, or equal temperature, for example). One of them is placed in the flow, while the other one is shielded from the flow, thus only reacting to the flow temperature. As both sensors give the same output in the absence of flow, the differential output for the sensor combination is a direct measure of the flow.

### 2.3 Electronic realization of thermal anemometers

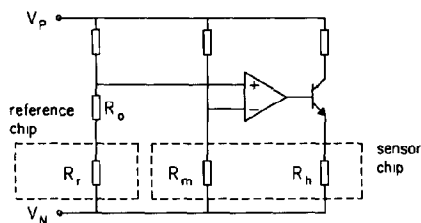
#### *Self-heating single-component thermal anemometers*

For its electronic operation, a thermal anemome-

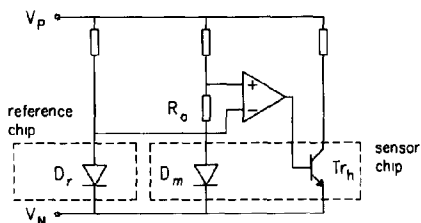
ter requires one or more electronic components for heating the sensor and measuring its temperature. This can be achieved with a self-heating resistive component like a thin metal wire or film [9–15]. The element is heated by the electrical current through it, and its temperature is determined from its electrical resistance. Hot-wire anemometers find special application in the measurement of very small flow velocities and fast velocity fluctuations (turbulent flow). For research probes the wires are normally made from platinum or tungsten, and have a typical length of 1 mm and a thickness of  $5\ \mu\text{m}$ . The heat transfer is mainly determined by the velocity component normal to the wire. For directional flow measurements multi-wire probes are used, with wires at different angles [11–14]. To improve the mechanical strength of the sensor, hot-film probes have been developed, which consist of a thin metal film deposited on a quartz tube. Semiconductor anemometers can be realized on this principle, using thermistors [16–18] or transistors [19–21], which have a much larger temperature sensitivity than metal resistors.

#### *Advanced microelectronic thermal anemometers*

Microelectronic thermal anemometers were first introduced by simply replacing discrete self-heating components by their integrated counterparts. Later, multi-component sensor structures were manufactured, where by using separate elements for heating and temperature measurement (in close thermal contact) an optimization of each function could be achieved [22, 23]. Figure 5 shows the circuit of a sensor that is heated by resistor  $R_h$ , while its temperature is measured by resistor  $R_m$ ,  $R_r$  is a temperature reference, and  $R_0$  sets the temperature elevation of the sensor. In Fig 5(b) a sensor is shown with heating transistor  $Tr_h$  and temperature-measuring diodes  $D_m$  and  $D_r$ . Other combinations are also possible, like bipolar temperature sensors with resistive heaters. Note that separate devices are required for the sensor and the reference, unless some form of thermal isolation can be created in the sensor. In the case of thin-film sensors, this can be achieved by using a special substrate of low thermal conductivity [24], whereas for monolithic silicon selective etching techniques exist which allow isolation structures



(a)



(b)

Fig 5 Multi-component anemometers with (a) resistive or (b) bipolar components

to be realized in the sensor chip, as will be discussed in Section 4

#### *Multi-sensor and direction-sensitive thermal anemometers*

Thermal anemometers typically respond to the absolute value of the flow velocity or of a velocity component. As mentioned previously, an additional sensor (or measurement) for temperature reference or to determine the flow-dependent output component is required. For direction-sensitive flow measurements, such as determining the sense of direction of the flow (one-dimensional) or measuring multiple orthogonal velocity components (two or three dimensional), even more complicated multi-sensor probes are required, where each sensor responds differently to the flow. These principles can also be applied in the design of multi-component flow sensors where several sensor elements are combined in a single device. To eliminate the flow-independent part of the sensor response, for example, an integrated Wheatstone bridge has been applied [25], which depends on the difference in cooling between the heated bridge elements that lie normal to the flow and those

parallel to it. As another example, directional flow measurements can be carried out by employing the difference in heat transfer between the upstream and downstream parts of the sensor. This can be implemented directly, in the form of a differential power measurement while keeping the sensor parts at equal temperature, or alternatively, by symmetrically heating the sensor and measuring the flow-induced temperature differences in it. By combining measurements in two directions normal to each other, a two-dimensional sensitivity is obtained, allowing both the velocity and the direction of the flow over the surface to be determined. Section 3 discusses silicon sensor structures that are based on this latter principle.

### 3. Direction-sensitive thermal flow sensors

A number of direction-sensitive thermal flow sensors have been reported in the literature, based on the measurement of flow-induced temperature differences in a chip [7, 24–32]. Depending on whether the temperature differences are measured in only one direction, or in two directions perpendicular to each other on the chip surface, the sensor can be regarded as having either one- or two-dimensional direction sensitivity. An overview of the research carried out at the Electronic Instrumentation Laboratory of Delft University of Technology on the development of one- and two-dimensional flow sensors made of silicon ICs is given in ref. 7.

#### *3.1 Operating principle of direction-sensitive flow sensors*

The heat transfer from a heated sensor to the flow is not distributed uniformly over its surface. At the upstream part the surface is cooled more strongly than at the downstream part, because a thermal boundary layer is built up with an increasing thickness when travelling downstream (see Fig. 6). Because of the finite thermal conductivity of the sensor, this differential cooling results in a temperature gradient in the sensor in the direction of the flow. Under the influence of the heat transfer to the flow, the temperature distribution, which is essentially symmetric at zero flow, becomes asymmetric.

#### *One- and two-dimensional flow sensors*

By measuring the temperature difference between

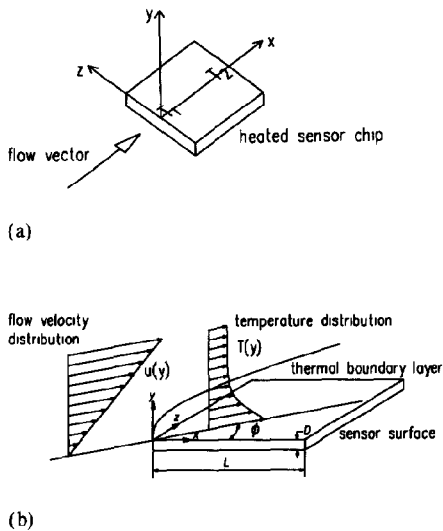


Fig 6 The operating principle of a direction-sensitive thermal flow sensor (a) Definition of the geometry, (b) thermal boundary layer development over a heated surface

two fixed points of the chip, a flow sensor results which is sensitive to flow components along the imaginary line that connects these two points. In the absence of flow, the temperature difference is zero. The sensor can detect flow reversal, because the polarity of the temperature difference reveals the sense of the flow direction, thus creating a one-dimensional sensitivity. When temperature differences are measured in two directions perpendicular to each other, both flow velocity and direction can be determined, and a two-dimensional sensitivity is obtained (see Fig 7)

In first approximation, the orientation of the thermal gradient is that of the flow direction, while the absolute value of the gradient depends only on the flow velocity. Hence, the temperature differences  $\Delta T_{12} = T_2 - T_1$  and  $\Delta T_{34} = T_4 - T_3$  are given by

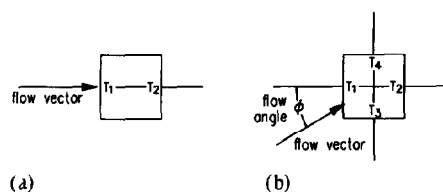


Fig 7 Thermal sensor based on the measurement of flow-induced temperature differences (a) one-dimensional and (b) two-dimensional sensitivity

$$\Delta T_{12} = \Delta T_0 \cos \phi \quad (7)$$

$$\Delta T_{34} = \Delta T_0 \sin \phi$$

The amplitude  $\Delta T_0$ , which is the temperature difference in the direction of the flow, is proportional to  $\Delta T$ , the average temperature difference between the sensor and the fluid, while further depending on the flow velocity

$$\Delta T_0 = F(U) \Delta T \quad (8)$$

The dimensionless sensitivity function  $F(U)$  expresses the dependence of the induced temperature differences on the flow velocity. In general,  $F$  includes the influence of the material properties of the fluid and the sensor (specific heat, conductivity and viscosity), and the geometry of the specific flow situation (shape and size of the probe in which the sensor is mounted) as well. For silicon sensors  $\Delta T_0$  is typically of the order of a few percent of  $\Delta T$ , because of the high value of the thermal conductivity of silicon.

The on-chip temperature differences  $\Delta T_{12}$  and  $\Delta T_{34}$  can be measured with thermopiles which have been integrated in the IC. By combining eqns (7) and (8), the corresponding thermopile output voltages  $V_{12}$  and  $V_{34}$  can be written as

$$\begin{aligned} V_{12} &= \alpha F(U) \Delta T \cos \phi \\ V_{34} &= \alpha F(U) \Delta T \sin \phi \end{aligned} \quad (9)$$

where  $\alpha$  is the thermo-electric sensitivity of the thermopiles, expressed in  $\text{V K}^{-1}$ . The flow angle  $\phi$  can easily be determined from the ratio of the two signals, and is insensitive to the exact form of the function  $F$ . This means that the flow direction angle can be calculated independently of the influence of the flow velocity on the temperature effects. The flow velocity can be determined from the 'amplitude' of the thermopile output signal, which is defined as  $V_0 = (V_{12}^2 + V_{34}^2)^{1/2}$ .

#### Thermal sensor model

A thermal sensor model has been used to calculate the temperature distribution  $T_s$  in the sensor surface as a result of the convective cooling [32]. The sensor is represented by a thin, rectangular surface element with lateral dimensions  $L \times W$  (let us assume that  $L = W$ ) and thickness  $D$ , which is thermally isolated from its substrate. A spatial coordinate system  $(x, y, z)$  is used as indicated in Fig 6, where  $x$  and  $z$  are surface coordinates,

while  $y$  is measured normal to the surface. When the variation of the temperature across the thickness of the sensor is neglected ( $D$  is assumed to be much smaller than  $L$  and  $W$ ), the momentary heat balance is given by

$$\rho_s c_s D \frac{\partial T_s}{\partial t} = k_s D \left( \frac{\partial^2 T_s}{\partial x^2} + \frac{\partial^2 T_s}{\partial z^2} \right) - q_f(x, z) + q_h(x, z) \quad (10)$$

where  $t$  denotes the time coordinate, and  $\rho_s$ ,  $c_s$  and  $k_s$  the density, specific heat and thermal conductivity of the sensor material. The terms on the right-hand side represent, respectively, the redistribution of heat due to lateral heat conduction, the surface heat transfer to the flow ( $q_f$ ) and the local heat production ( $q_h$ ). Both  $q_f$  and  $q_h$  are expressed per unit area. The heat production is assumed to be distributed uniformly over the sensor surface. Assuming the temperature variations over the surface to be small,  $q_f$  can be approximated as the heat transfer from an isothermal surface ( $T_s = \text{constant} = T_{\text{amb}} + \Delta T$ ). When further the thermal boundary layer is confined to the lower region of the velocity boundary layer over the surface, the situation is comparable to that of Fig 2(b). The flow field is then characterized by the local surface shear stress  $\tau_s$ , and the heat transfer is given by eqn (4)

#### One-dimensional solution of the sensor model

For  $\phi = 0$  the temperature distribution depends only on the streamwise coordinate  $x$ , and for this one-dimensional case the steady-state solution is easily obtained by integrating eqn (10) twice with respect to  $x$ . Upon substitution of eqn (5), the flow-induced temperature difference  $\Delta T_0 = T_s(L - x, z) - T_s(x, z)$  between two points located symmetrically on the sensor surface with respect to the centre line  $x = L/2$ , is found to be

$$\Delta T_0 = c \frac{L}{k_s W D} G_f \Delta T \quad (11)$$

where  $c$  is a constant, which has a maximum value when the points are located at the opposite edges of the sensor (in that case  $c = 1/10$  for shear flow). Note that eqn (11) can be interpreted as the product of the thermal resistance of the sensor  $L/(k_s W D)$  and the total convective heat flow

$G_f \Delta T$ , where  $c$  is a kind of efficiency parameter depending on the distribution of the heat transfer over the surface and on the location of the measurement points.

For practical applications it may be desirable to be able to express the sensor operation in terms of a characteristic flow velocity  $U$ , such as the velocity of the undisturbed flow field far upstream of a sensor probe. As the relation between  $G_f$  and  $U$  is determined by the boundary layer over the sensor, this relation obviously depends on the probe geometry, and no universal relation can therefore be given. For geometrically similar laminar boundary layer flows, it is, however, possible to derive by dimensional analysis (see also the results of the discussion in Section 2.1) the following result [8]

$$\frac{\Delta T_0}{\Delta T} = K_s K_p Pr^{1/3} Re^{1/2} \quad (12)$$

where  $K_s$  is a sensor geometry factor,  $K_p$  an overall probe geometry factor,  $Pr = \nu/a$  the fluid Prandtl number, and  $Re = UL/\nu$  is Reynolds number. Comparison of eqns (8) and (12) shows that  $F(U) \propto U^{1/2}$ , i.e., the sensor output increases with the square root of the flow velocity. This relation has been derived under the assumption of laminar boundary layer flow. For turbulent flow the parameters  $K_s$  and  $K_p$  are different, while a value somewhat smaller than  $1/2$  is found for the exponent of  $Re$  [33].

The solution which has been derived above expresses how the thermal signal is related to the relevant flow parameters, and yields what explicit form should be expected for eqn (8), which describes the one-dimensional sensitivity (the velocity dependence). To analyse the flow direction dependence in order to verify eqn (7), the full two-dimensional solution of eqn (10) should be evaluated. The results of a numerical solution of this problem support the use of this simple expression, which was confirmed by experiments [32].

Analysis including the effect of the time-dependent term reveals that the response of the temperature distribution to a stepwise change in flow direction can be approximated with an exponentially decaying response function, for which the time constant is equal to  $c_s \rho_s L^2 / k_s \pi^2$ , showing the response speed to be determined by the lateral conduction of heat in the surface.



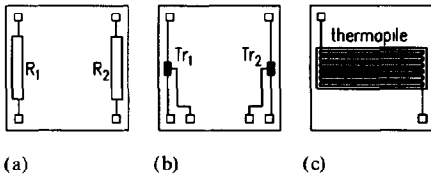


Fig 8 Electronic components for integrated direction-sensitive flow sensors (a) resistor pair, (b) bipolar transistor pair, (c) integrated thermopile

### 3.2 Description of the sensors

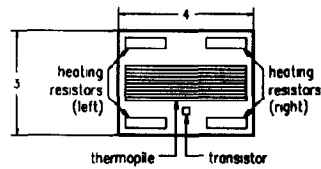
#### Electronic measurement of the on-chip temperature differences

Integrated components which are suitable for the measurement of on-chip temperature differences are resistor bridges, differential bipolar transistor pairs and thermopiles. The schematic layouts for sensors relying on these principles are depicted in Fig 8, for a one-dimensional sensitivity.

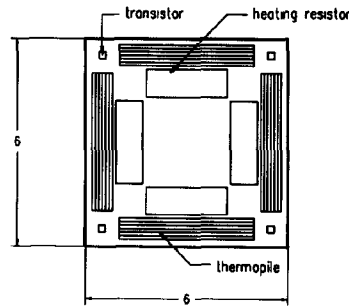
Temperature-difference sensors based on a modulating effect (such as a resistor bridge or a differential transistor pair) suffer from electronic offset and offset drift. Even if there is no temperature difference, an offset signal may be present because of the mismatch in the individual components due to their large spatial separation. The problem of offset can be avoided by using a temperature-difference sensor relying on a self-generating effect, such as a thermopile. The output voltage  $V_o$  of a thermopile is equal to  $(N\alpha_s \Delta T_o)$ , where  $N$  is the number of elements in the thermopile,  $\alpha_s$  the Seebeck coefficient and  $\Delta T_o$  the temperature difference between the ends of the thermopile. The Seebeck coefficient  $\alpha_s$  is a material constant, which for an integrated thermopile made of diffused p-type silicon strips and aluminium interconnection strips equals  $0.5\text{--}1.0\text{ mV K}^{-1}$ , depending on the exact doping concentration of the silicon. This type of integrated thermopile can easily be fabricated in standard IC processes [34, 35].

#### Layout of the ICs

The layout and the dimensions of one- and two-dimensional IC flow sensors are shown in Fig 9. The sensor ICs have a thickness equal to that of the silicon wafer out of which they are manufactured ( $0.35\text{ mm}$ ), and were processed in a fully standard bipolar process. The one-dimensional flow sensor measures  $3\text{ mm}$  by  $4\text{ mm}$  and contains a number of heating resistors, a bipolar transistor



(a)



(b)

Fig 9 Schematic layout of thermal IC flow sensors (dimensions are in mm) (a) one-dimensional sensor, (b) two-dimensional flow sensor

to measure the average temperature, and an integrated thermopile to measure the flow-induced temperature differences. The thermopile consists of 20 interconnected strips of DP-type diffused Si, and has an estimated sensitivity of  $12\text{ mV K}^{-1}$ , while having an internal resistance of approximately  $18\text{ k}\Omega$ . Separate heating resistors are present for the left and right parts of the sensor (nominal resistance value is  $80\text{ }\Omega$  each), to enable the heating of the sensor to be balanced. This provides a means to eliminate the thermal no-flow offset, i.e., the removal of temperature differences that occur at the absence of flow due to thermal asymmetries in the sensor assembly.

The two-dimensional flow sensor (see also Fig 10) measures  $6\text{ mm}$  by  $6\text{ mm}$  and has four separate heating resistors ( $450\text{ }\Omega$  each) to allow the heating to be balanced in both measurement directions. The sensor further contains (four) bipolar transistors to measure the average sensor temperature, while four integrated thermopiles (each consisting of 11 strips of diffused DP-type Si) are situated along the sides of the chip to measure the flow-induced temperature differences in two directions perpendicular to each other. For each measurement direction the two parallel thermopiles are connected in series, resulting in a

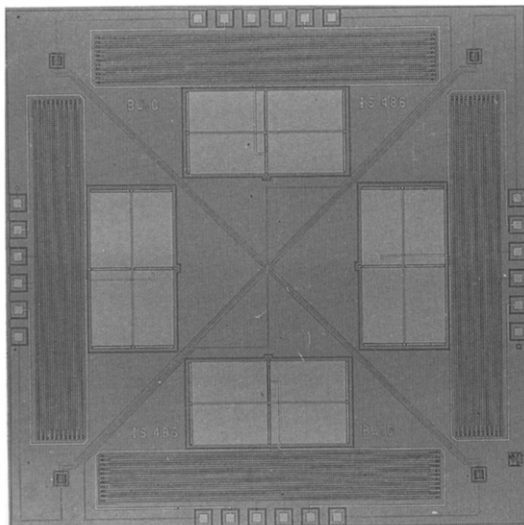


Fig 10 A two-dimensional flow sensor with thermopiles to measure the flow-induced temperature differences

total sensitivity of  $13 \text{ mV K}^{-1}$  and an internal resistance of  $18 \text{ k}\Omega$

### Sensor assembly

The mounting of the IC sensor used for flow measurement experiments is illustrated in Fig 11 (The subject of sensor assembly will be discussed in more detail in Section 6) The sensor chip has been bonded to a  $0.25 \text{ mm}$  thin ceramic carrier substrate (lateral dimensions  $25 \text{ mm}$  by  $25 \text{ mm}$ ),

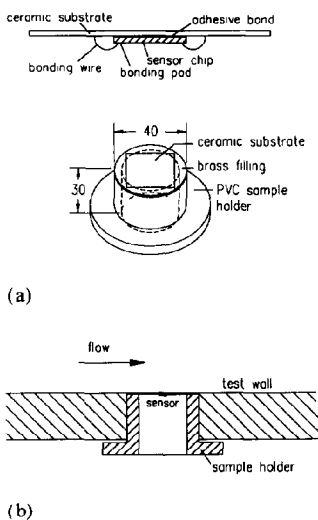


Fig 11 Sensor assembly, not to scale (a) mounting of the chip to the carrier substrate and assembly of the sample holder, dimensions are in mm, (b) cross section of the sample holder in the flow set-up

and this substrate is exposed with its other side to the flow. In this way a smooth flow surface is obtained, while the silicon sensor itself is shielded from the fluid. Standard wire bonding was used to contact the sensor to the metal interconnection pattern on the ceramic. In fact, the substrate now functions as the actual sensing area. Because of its relatively large dimensions ( $25 \text{ mm}$ ) and small conductivity ( $30 \text{ W/K m}$ ), the substrate determines the time response of the sensor, which has been measured to be of the order of  $2 \text{ s}$ , whereas the theoretical time response of the silicon IC alone is only about  $40 \text{ ms}$  [32]. The response speed is sufficient for the application of measuring average flow velocities.

A thermal isolation structure of the total sensor device has been provided by attaching the ceramic substrate only at its edges to a PVC sample holder, creating an air chamber around the silicon sensor. In this way the contribution of the conduction to the sample holder is kept small; the increase in heat transfer after the assembly had been attached to the sample holder was measured to be less than  $10\%$  of that of the chip-to-substrate assembly alone. For flow measurements the sample holder is fitted into a circular opening in the test plate, over which a well-defined air flow can be established (Fig 11(b)). To obtain a smooth flow surface, the upper surface of the device is aligned accurately with that of the plate. The direction sensitivity of the sensors was measured by rotating the sample holder around its axis, thus changing the relative flow direction.

### Electronic operation

An electronic circuit similar to that of Fig 5(b) was used for the temperature control of the sensor, and has been described in more detail elsewhere [32]. The sensor and flow temperatures are measured with transistors on the sensor chip and on a similar unheated reference chip respectively. The temperature measurement relies on the change with temperature of the base-emitter voltage of a transistor at constant current, which was measured to be  $-2.1 \text{ mV K}^{-1}$ . By means of a feed-back amplifier, the value of the heating current is adjusted so as to maintain a constant temperature elevation of the sensor (typically of the order of  $10\text{--}20 \text{ K}$ ). The heating of the sensor was balanced so that the temperature differences are zero in the absence of flow.

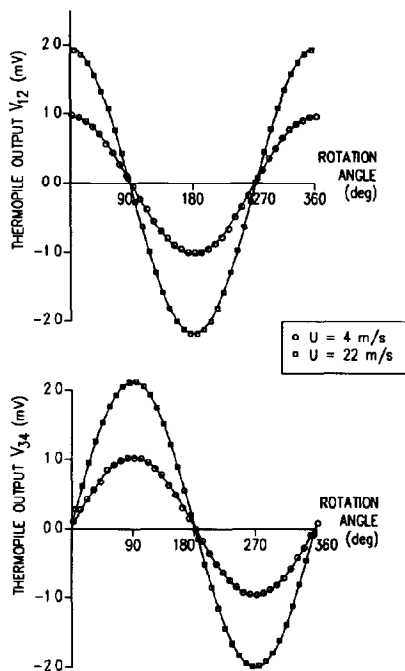


Fig 12 Thermopile voltages as function of flow angle (wafer-thick sensor,  $\Delta T = 17$  K)

### 3.3 Experimental results

Sensor calibration tests have been performed with a turbulent boundary-layer flow present over the test plate. Figure 12 shows the result of the rotation of the probe at two flow velocities, corresponding to the sensor model, eqn (9), within  $1^\circ$  in angle and 1% in amplitude. The variation of the thermopile voltages is given by harmonic curves, the amplitude of which increases with the flow velocity. The remaining thermal offset in the presence of flow, which results in a small vertical displacement of the curves with respect to the zero level, is limited to about 2 to 5% of the signal amplitude  $V_0$ . The total heat loss and the flow-induced temperature difference, divided by the temperature difference  $\Delta T$ , have been plotted in Fig 13 as a function of the square root of the flow velocity for three different sensor samples. For one sample two calibrations have been given, for  $\Delta T = 12$  and  $17$  K, which were obtained at a time interval of six months, showing an excellent reproducibility and long-term stability of the sensor. Note that, as the sensitivity of the thermopiles is equal to  $\alpha = 13$  mV K $^{-1}$ , the value of the relative flow-induced temperature difference  $\Delta T_0/\Delta T$

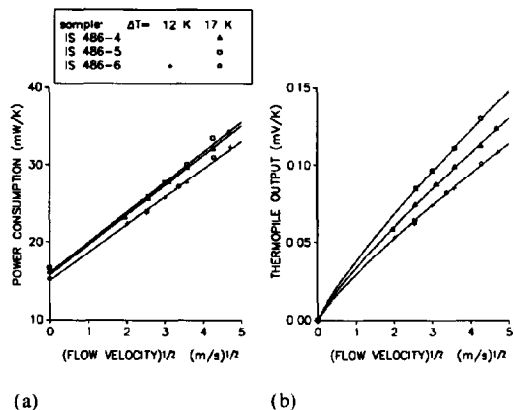


Fig 13 Sensor characteristics as a function of flow velocity (a) total power consumption, (b) induced temperature gradient (thermopile output), functions have been scaled with the temperature difference between sensor and flow

amounts to no more than 0.01 for  $U$  up to  $25$  m s $^{-1}$ . The small non-linearity in the curves is caused by the effect of turbulence. Fitting the measurement data to a simple power function in  $U$ , the value of the temperature difference  $V_0$  is found to increase with  $U^{0.42}$ . Note that the value of the exponent differs only slightly from the theoretical result of 0.5 for laminar flow.

## 4. The use of micromachining for flow sensor applications

The flow sensors that have been discussed all consist of devices which are integrally heated. The thermal isolation of such bulk devices depends on their mounting, which is often difficult to control. Also, their large thermal mass results in a slow time response, typically of the order of several seconds. With the selective etching of silicon, small thermally isolated areas that act as the actual sensing part can be created in a device, resulting in improved sensitivity and time response.

### 4.1 Silicon micromachining

Silicon sensors with special three-dimensional structures can be fabricated by the use of special etching techniques which are used for the selective removal of the silicon [36]. This way of creating

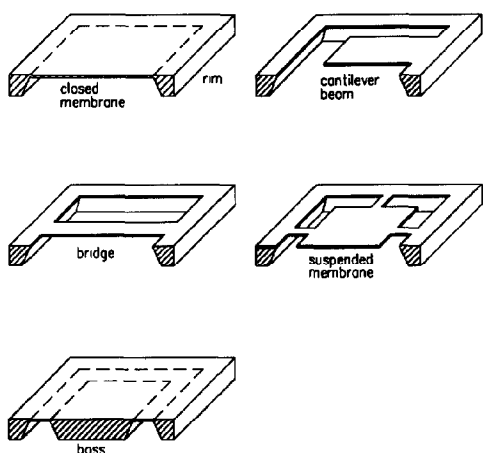


Fig 14 Some basic sensor structures that can be obtained with silicon micromachining

miniature mechanical geometries is usually referred to as micromachining. Etching can either be performed by exposing the silicon to an etching liquid (wet etching), or by means of a plasma (dry etching). Further, we can distinguish between bulk micromachining from the back of the device and surface micromachining using undercut etching or sacrificial layer techniques. Silicon etching techniques have been used extensively for the realization of mechanical and thermal sensors.

In Fig 14 a number of easily achievable structures are shown, which are compatible with standard planar processing. This compatibility means that the etching steps can be performed separately, after completion of the planar process in which the electronic components of the sensor have been realized. The simplest structure is formed by a closed membrane. In a square area in the centre of the chip the major part of the silicon has been etched away from the back of the chip, leaving only a thin diaphragm at the surface with a thickness of typically a few microns. By etching away parts of the membrane surface as well, cantilever beams, bridges and suspended membranes can be formed. Flow sensors of this structure require the sensor to be exposed with its component side to the flow. A slightly different type is the bossed structure, where etching is performed only to achieve thermal isolation, but where the sensor part (the island in the centre) is maintained at its original thickness. This structure is used for flow

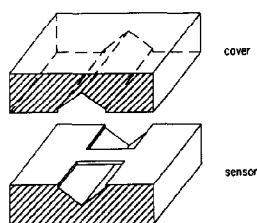


Fig 15 Microchannel device with a sensor bridge suspended over an etched groove, the channel structure is completed by a cover wafer which is bonded to the sensor wafer

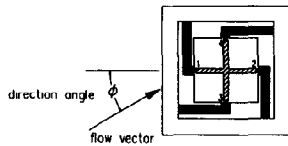
sensor applications where the sensor is exposed with its back to the flow.

Several thermal flow sensors have been reported in the literature in which small, thermally isolated sensing areas have been created within the chip [37–51]. Indeed, all of the above structures have been employed: closed membrane [37, 38, 44, 50], bridge [42, 47, 48, 49, 51], cantilever [39, 40, 45], suspended membrane [43, 46] and bossed structure [41]. In a number of applications, the sensors are intended for use in miniature flow channels which are formed in the chip itself [47–51], see Fig 15. Electronic components can be integrated in the remaining structure if it consists of monocrystalline silicon. A number of silicon sensors have been reported where all the silicon was etched to increase the thermal isolation even further, using a dielectric material (porous silicon, silicon dioxide or silicon nitride) as mechanical carrier of the anemometer components, in this case thin-film or polysilicon resistors are used.

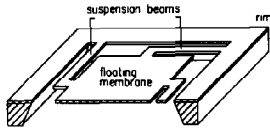
#### 4.2 An etched two-dimensional flow sensor

In Fig 16 a two-dimensional flow sensor is shown, where a thin floating membrane has been formed which is suspended with thin beams from the solid rim [46]. The membrane functions as the actual heated sensing area. As in the case of the wafer-thick sensors described before, the flow measurement is based on the detection of flow-induced temperature differences in two directions normal to each other.

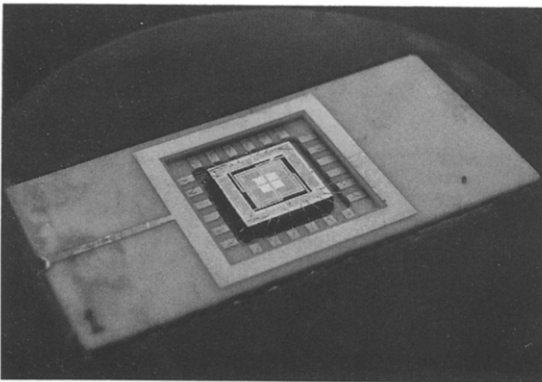
A structure like this has a number of advantages when compared to a solid (i.e., of wafer thickness) flow sensor of similar lateral dimensions. The value of the induced temperature differences is inversely proportional to the sensor thickness,



(a)



(b)



(c)

Fig 16 Floating-membrane direction-sensitive thermal flow sensor (a) lay-out, (b) cross section of the sensor, (c) photograph of the mounted chip

and, hence, the thermal sensitivity is strongly increased (theoretically, by a factor of about 30, being the ratio of the thickness of the wafer to that of the membrane) Further, the greatly reduced heat capacity of the sensing element increases the overall response speed of the device, while the effective isolation results in small conductive heat losses As the thermal isolation of the sensor is no longer determined by the mounting of the chip but by its structure, this effectively reduces the thermal offset The high signal-to-offset ratio makes the sensor suitable for the detection of very small flow velocities A further advantage of the thermal isolation structure is the possibility of using the rim as a reference for the ambient temperature, resulting in a one-chip sensing device, whereas a solid sensor requires a separate reference sensor

### Layout, fabrication and assembly

The total size of the sensor is 6 mm by 6 mm, while the membrane area measures 3.4 mm by 3.4 mm Each beam contains two thermocouple elements to measure the average temperature elevation of the membrane relative to the rim, which are all connected in series The resulting eight-element thermopile has a total estimated sensitivity of 5 mV/K and an internal resistance of 13.6 k $\Omega$  Two thermocouples measure the flow-induced temperature differences in the membrane, each having a sensitivity of 1 mV/K and a resistance of 10.6 k $\Omega$

The devices were processed in a slightly modified bipolar process, in which the heating resistors and the p-type diffusion thermopiles were created Subsequently the floating membrane structure was created in a two-step micromachining process In the first step a 4 mm by 4 mm square membrane was electrochemically etched from the back of the wafer, which is 10  $\mu\text{m}$  thick (equal to the thickness of the epilayer) The etch process is controlled to stop automatically at the epilayer-substrate junction, which is in reverse bias Out of this closed membrane the floating membrane and the suspension beams were formed by means of plasma etching The membrane measures 3.4 mm by 3.4 mm, and the beams are approximately 2 mm long and 150  $\mu\text{m}$  wide

The sensor was mounted in a ceramic housing with the component surface of the chip level with that of the housing (see Fig 16) In the preliminary flow measurements no special care has yet been taken to eliminate the possible disturbing effects of the gap around the sensor and of the bonding wires However, even with this configuration very promising results have been obtained

### Experimental results

The power consumption of the sensor at zero flow was measured to be 1.45 mW/K, which consists mainly of the conduction in the beams (estimated to be about 0.5 mW/K), and the conduction in the air gap under the membrane (about 0.9 mW/K) For directional flow measurements the sensor assembly was mounted in the same test set-up as that used for the solid sensors described in Section 3 The membrane was heated with respect to the rim to an average temperature elevation of 17 K In Fig 17 the measured thermocouple output voltages  $V_{12}$  and  $V_{34}$  are shown as a

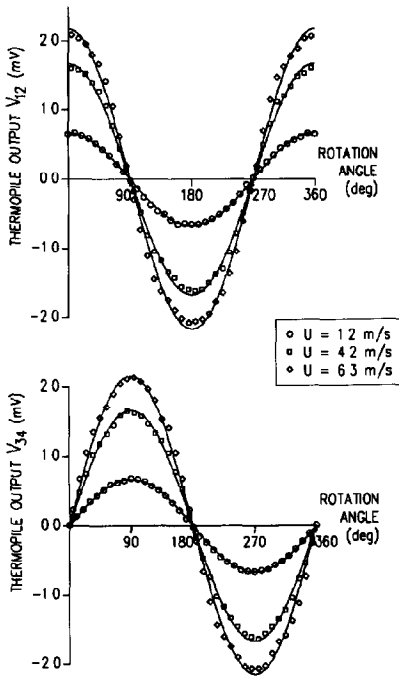


Fig 17 Thermopile voltage as function of flow angle (floating-membrane sensor,  $\Delta T = 17$  K)

function of flow direction, for three different flow velocities. The amplitude of the calibration curves was found to increase in proportion to the square root of the flow velocity, to the extent of  $0.8 \text{ mV} (\text{m/s})^{-1/2}$ . The thermal sensitivity (i.e.,  $\Delta T_{12} \Delta T^{-1} U^{-1/2}$ ) is equal to  $0.05 (\text{m/s})^{-1/2}$ , which is about 25 times as high as that of a wafer-thick sensor of comparable size. At the lowest flow velocity, the deviations from the modelled behaviour are  $1^\circ$  in flow angle and 2% in amplitude, over the full range of  $360^\circ$ . At higher velocities the differences were found to increase to  $3^\circ$  and 5%, respectively, and result from a systematic deviation from the harmonic curves. Possibly edge effects due to the square geometry of the sensor (which were less pronounced for the wafer-thick sensors because of the presence of the ceramic substrate) and the disturbance of the flow because the sensor assembly is not completely smooth can be held responsible for this.

The response time for a step change in heating power was measured to be 150 ms at zero flow (and decreases with increasing flow velocity). This finding is in good accordance with the theoretical time response obtained from a lumped sensor

model, based on the calculated heat capacity of the membrane ( $0.2 \text{ mJ/K}$ ) and the measured total heat-transfer rate ( $1.45 \text{ mW/K}$ ), yielding a value of 140 ms. It should be noted, however, that the flow measurement is not based on the average temperature of the membrane, but on the flow-induced temperature differences in it. The time response for this latter mode can be estimated to be only 15 ms, which is one order smaller than that of the average temperature behaviour. The time response is sufficient to allow the detection of turbulent velocity fluctuations in the flow, and to observe flow transition. This is illustrated by the oscillograph in Fig 18, which shows the simultaneous measurement of  $V_{12}$  (upper curve) and  $V_{34}$  (lower curve). The flow angle is equal to zero, so that  $V_{12}$  responds mainly to velocity fluctuations, while  $V_{34}$  is especially affected by variations in the flow direction. The flow situation is that of laminar flow with occasional turbulent bursts, which can clearly be identified in the sensor response.

## 5. Applications: an electronic wind meter

After having discussed the structure and operation of thermal flow sensors, we turn our attention here to their application. A specific example is described, namely that of an electronic wind meter without moving parts, for the measurement of

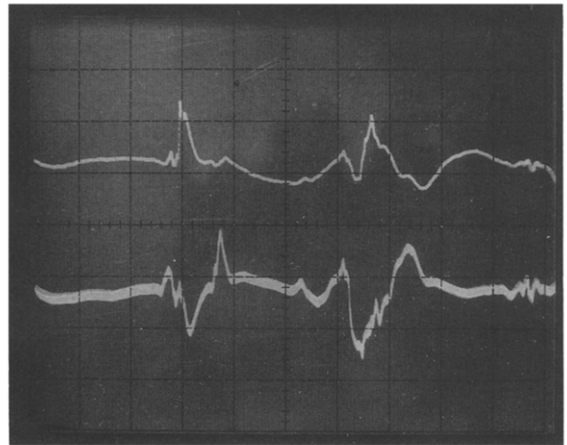
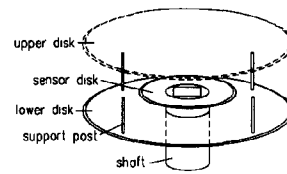


Fig 18 Oscillograph of the thermopile output voltages  $V_{12}$  (upper curve) and  $V_{34}$  (lower curve). Horizontal scale time, 0.1 s per division. Vertical scale voltage, 0.1 mV per division.

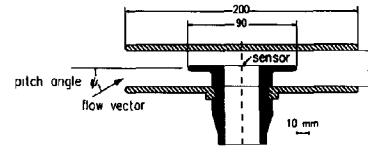
(horizontal) wind speed and direction [52] Such an electronic wind meter can be used in combination with sensors for other meteorological variables in an automated weather station To be able to use the sensor as a wind meter, it must be incorporated in a suitable probe body The shape of the probe should be such that the flow over the sensor is representative of the horizontal wind flow, while having a  $360^\circ$  sensitivity in obtaining the wind direction angle  $\phi$  Also, it should not be sensitive to vertical wind components and pitch The pitch angle is defined as the angle between the flow velocity vector and the horizontal plane of the sensor In addition, the probe should protect the sensor against disturbing external influences, such as direct sunshine or precipitation, and against handling damage

The simplest rotational probe form would be a flat disk mounted on a vertical shaft with the sensor mounted in the flat upper surface of the disk (indicated by the densely hatched areas in Fig 19, see also Fig 1) Apart from the vulnerability of this configuration, this shape is unsuitable because of its high sensitivity to pitch Figure 20 shows how even moderate changes of the pitch angle have a strong influence on the sensor output Large negative values occur when the probe is tilted only slightly backwards, because a region of reversed flow is formed due to flow separation (stall effects) A suitable probe shape has been obtained by placing large circular disks below and above the central body to guide the flow In this way, the effective pitch angle of the sensor body is reduced strongly, while the sensor is further protected by the upper disk

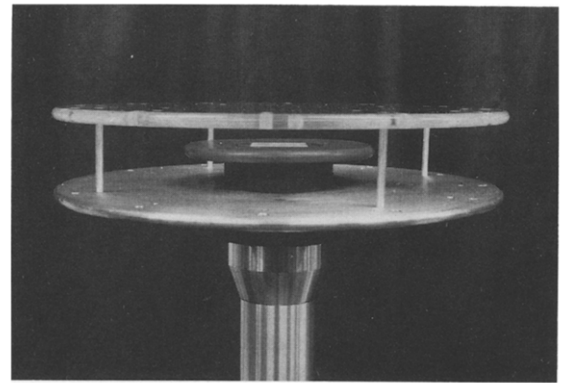
The prototype has been tested in a steady wind flow for velocities up to 25 m/s Rotation tests showed that the deviations were slightly larger than for the sensor experiments described in Section 3.3, which can probably be attributed to inaccuracies in the shape of the probe The maximum error was found to be about  $2^\circ$  in angle and 2% in amplitude, provided the flow can travel unhindered over the sensor Measured velocity characteristics have been plotted in Fig 21 The change in the slope of the curve at a wind speed of approximately 6 m/s corresponds to the transition from laminar to turbulent flow for the boundary layer over the sensor body This is caused by the rather blunt shape of the sensor disk (for ease of



(a)



(b)



(c)

Fig 19 Wind meter design (a) perspective view, not to scale, (b) cross section, (c) photo of the prototype model

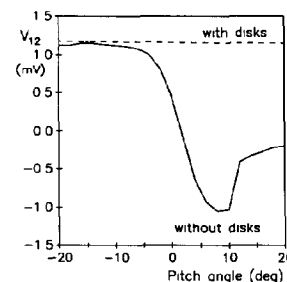


Fig 20 Influence of pitch angle on the wind meter output

manufacture a semicircular edge was applied), and can be eliminated from the range of practical wind speeds by applying a more streamlined shape In the laminar-flow region of the calibration, the output is proportional to the square root of the flow velocity as predicted by the theory The sensitivity

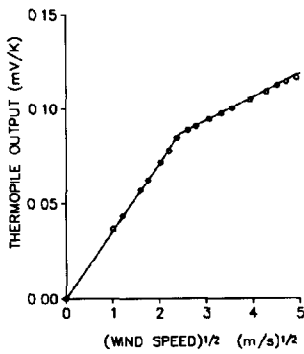


Fig 21 Wind meter characteristic sensor output as a function of flow velocity

of the measurement, which is defined as  $V_{12} \Delta T^{-1} U^{-1/2}$ , was determined to be  $35 \mu\text{V/K} (\text{m/s})^{-1/2}$ . As the thermopile sensitivity is equal to  $13 \text{ mV/K}$ , the thermal sensitivity  $\Delta T_{12} \Delta T^{-1} U^{-1/2}$  of the sensor structure amounts to  $0.0027 (\text{m/s})^{-1/2}$ . For a sensor operated at  $\Delta T = 20 \text{ K}$ , the typical thermal offset was observed to be  $20 \mu\text{V}$ , so that, accordingly, the flow detection threshold can be estimated to lie below  $1 \text{ cm/s}$ .

In the prototype the upper disk was connected with cylindrical posts with a diameter of  $2 \text{ mm}$ . When the flow direction is such that one of the posts is in the path of the flow over the sensor, considerably larger errors occur than those mentioned above, due to the wake of the cylinder (resulting error  $\pm 5^\circ$  in angle and  $-10\%$  in amplitude). Therefore, thin posts or preferably a grid or screen of thin wires should be used. Good results were obtained with a fine metal screen of  $60\%$  relative open area.

## 6. The packaging of silicon thermal flow sensors

The packaging of integrated silicon structures used as sensors is a topic that requires special attention [53, 54]. In any application the way in which the sensor is mounted will certainly influence and may even determine the overall sensor performance. In the case of 'standard' ICs, used for purely electronic applications, the packaging involves mounting the device to a carrier, making electrical contacts and protection by sealing it from the environment as much as possible. Silicon sensors, however, fundamentally require an inter-

action with their environment in order to perform their sensor function. As a result, this often calls for non-standard packaging and assembly techniques, which may be very much dependent on the type of sensor and its application. Radiation sensors, for example, would only require that the package be transparent to the relevant radiation, thermal sensors can be covered with a protective, but thermally conductive, coating, whereas for chemical sensors a direct contact with the medium is a prerequisite. The choice of the package and the design of the sensor assembly are dominated by the following considerations:

- sensor performance (strong and reproducible interaction with the environment),

- reliability (protection and mechanical strength),

- cost (non-standard packages and assembly techniques are expensive).

With reference to thermal flow sensors, this means that the following aspects of the complete sensor assembly (including sensor device and housing) must be considered:

- aerodynamic the incorporation of the sensor in the system such that correct and reliable operation is obtained, the permissible disturbance of the flow,

- thermal heat conduction in the package, thermal inertia and response time,

- mechanical all elements of the sensor and package should have sufficient mechanical strength to withstand the static and dynamic loads that may be encountered,

- electronic contacting of the sensor and connection to external systems,

- chemical resistance to corrosion, influence of pollution and moisture.

A number of possible assemblies are shown in Fig 22, which also indicates the types of micro-mechanical configurations the specific assembly allows to be used, namely the thin-membrane type when the component side of the sensor is exposed to the flow, or only bossed-type structures when the back-side of the sensor is used.

### (a) Standard mounting with encapsulated bonding wires

When the flow is predominantly from one direction, the bonding wires can be located at the sides of the sensor area, or downstream of it, so that they do not disturb the flow over the sensor. The bonding wires can be covered by a protective



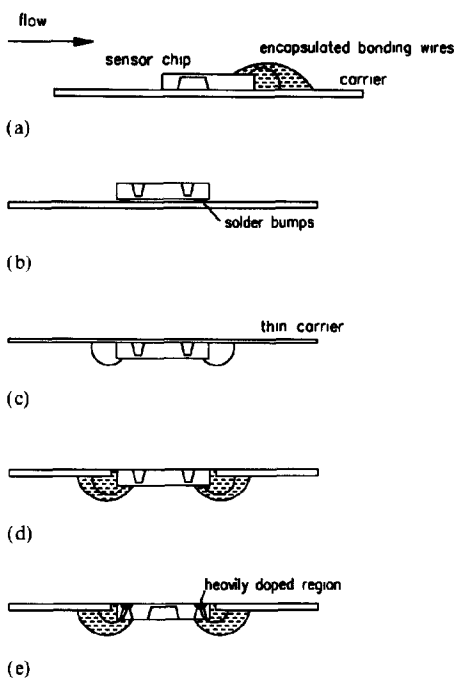


Fig. 22 The assembly of silicon thermal flow sensors

polymer encapsulation. This type of mounting has been used for chemical sensors [54] and also in catheter-type flow probes [37, 40]

#### (b) Flip-chip bonding

The use of the flip-chip mounting eliminates the fragile bonding wires. No specific reference to this type of mounting in connection with thermal flow-sensor applications is known to the author.

Both (a) and (b) result in configurations that do not present a flat surface to the flow. With some effort the surface steps can be reduced, but it is unlikely that a very smooth surface can be obtained. The following three configurations do not have this problem.

#### (c) Reversed configuration with thin carrier

The sensor chip is mounted on a thin sensing and carrier substrate, which is exposed with its back to the flow. This configuration, which has been used for the experiments described in Section 3, combines a flat surface with the use of standard mounting and bonding techniques, simultaneously providing a protection layer between sensor and fluid. The choice of the carrier is determined by a compromise between sensor performance and me-

chanical strength. Micromechanical structures are possible only in the form of bossed structures, and on the condition that the lateral conduction in the carrier is small. This calls for a carrier of low thermal conductivity and small thickness.

#### (d) Reversed embedded chip in carrier with hole

In this configuration a carrier is used which has an opening to accommodate the sensor. The assembly is made by putting sensor and carrier upside down on a flat surface, and then making the electrical and mechanical connection between sensor and carrier. The realization is more complex than that of (c), but now the chip is in direct contact with the flow, whereas there are less severe demands on the carrier material and dimensions. The configuration allows the use of bossed structures, and has been applied for a sensor to measure fouling biofilms in liquid flow [41]. Configurations (c) and (d) can be combined by first mounting the sensor to a very thin film, which is then attached to the flat face of a package with an opening in it.

#### (e) Embedded chip with back-side contacts

This configuration shows the very favourable combination of a flat surface and the possibility of exploiting the high sensitivity of thin sensing structures. Contacting is achieved by forming heavily doped contact regions which are reached by etching holes from the back of the sensor. This special technique has been reported for use in chemical sensors [54, 55].

As stated earlier, which of these configurations is the most appealing for a specific application depends to a large extent on the specific circumstances (gas or liquid flow, level of mechanical loads, corrosive nature of the environment), on the required sensor performance and on the aspect of cost.

## 7. Obstacles in the signal transduction path

After having discussed the various aspects of the design and application of silicon thermal flow sensors, let us now return again to the more general view of the complete transduction path, as illustrated in Fig. 1. The complete signal chain goes from the relevant flow parameter to be measured (say, wind speed) to an electrical signal. It is evident

that any obstacle in the transduction path will cause an erroneous measurement a 'perfect' instrument that fails to deliver a signal, and a 'perfect' electrical transducer in an inappropriate housing may be equally useless. Apart from the possibility of such catastrophic obstacles, which should be eliminated by proper design and use, smaller barriers of various natures are always present. These limit the transduction accuracy, and hence, determine the performance of the entire measurement system. Important performance-limiting effects are noise and offset. Noise is the occurrence of natural, spontaneous fluctuations in a signal and sets a lower bound for distinguishing input signal variations. Offset is defined as the presence of undesirable signal components in the sensor output, due to effects other than a change in the measurand. As the thermal flow sensor is a tandem transducer (mechanical-thermal-electrical), it is again possible to distinguish electronic, thermal and mechanical aspects. Let us consider again the sensor and its application that we have discussed previously.

#### *Electrical domain*

Electronic offset occurs in the measurement of the on-chip temperature differences when a modulating transduction principle is used, as in the case of a differential transistor pair or a resistor bridge. A non-zero electronic output signal (offset) can exist in the absence of a temperature difference, due to variations in the characteristics of the individual components (transistors, resistors) and, e.g., due to mechanical stresses in the sensor. In this respect the use of a passive (self-generating) thermal transducer, such as a thermopile, is to be preferred. As such sensors rely on a self-generating effect, they are inherently offsetless, and the problem of electronic offset and drift is eliminated to a large extent, the overall performance being limited by thermal noise and interference. For a typical integrated thermopile, the noise-equivalent temperature difference is of the order of only  $1 \mu\text{K}$  [34]. For most applications this is sufficiently small, and the limits to the overall sensor performance will be dominated mainly by thermal and mechanical causes.

#### *Thermal domain*

Thermal offset can be defined as the temperature difference on the sensor in the absence of

flow, or when the flow is perpendicular to the specific measurement direction of the sensor. It may result from the asymmetry in the sensor caused by inhomogeneities in it and by mismatch in the heating-resistor values, which would cause an uneven distribution of the heating power over the sensor. Probably the largest source of thermal offset lies in inhomogeneities in the mounting of the IC sensor to its housing or substrate. As discussed previously, the presence of separate heating resistors provides an opportunity to control the distribution of the heating power over the sensor surface, and in this way a thermal balancing of the sensor can be realized.

#### *Mechanical domain*

As the operation of the sensor as a flow sensor is based on the existence of an unambiguous relation between the heat transfer from the sensor and the flow property which is to be measured, measurement errors arise when the heat transfer is not sufficiently representative of the normal flow situation. A non-zero temperature difference can then occur even if there is no flow, or when the flow is perpendicular to the measurement direction. This can happen, e.g., under the influence of natural convection when the sensor is operated normally in a horizontal position and is then tilted with respect to the vector of gravity, a natural convection flow will induce a temperature gradient on the sensor. This effect is important only for the low velocity range (flow speeds below  $1 \text{ m/s}$ ). For a temperature elevation of the sensor of about  $20 \text{ K}$ , the maximal effect, occurring when the sensor is placed vertically, corresponds to a flow velocity of the order of only a few  $\text{cm/s}$ .

A second example of mechanical offset is the case when the boundary layer flow is laminar over one part of the sensor and turbulent over the other. As the heat transfer in the turbulent flow will usually be larger than that in the laminar flow, this will result in an erroneous interpretation of the flow angle and velocity.

## **8. Towards smart flow sensors**

The main subject of attention in this paper has been the physical transduction effects. We have

discussed the thermal transduction which takes place in the sensor in depth, and have considered aspects concerning a practical application. With regard to the electrical domain, we have been satisfied to see how electronic components can be employed to measure the thermal signal, like the use of thermopiles to measure temperature differences on the chip. Apart from the use of microelectronic techniques to manufacture special structures, the silicon sensor resembles other classic thermal flow-sensor types, in that it delivers an analog output signal where the information-carrying signal is an electric voltage or current. However, one of the important motives to stimulate silicon sensor research is the possibility of including electronics for signal conversion on the sensor device [56], ultimately to achieve so-called smart sensors. A serious treatment of all aspects involved merits a publication to itself, and is not attempted here, but let us make some brief remarks on the possible strategies that allow sensors with special output signal structures to be realized.

#### Signal conversion in the electrical domain

By means of an electronic conversion, a duty cycle, pulse width, frequency or digital output signal can be obtained. As an example, Fig 23 shows a frequency converter for a two-dimensional flow sensor of the type discussed in Section 3 [57, 58]. It is based on a relaxation-type oscillator, by periodically charging and discharging capacitor  $C$  with a current proportional to the sensor output voltages. When the capacitor voltage  $V_C$  reaches the positive threshold limit, the comparator switches the choppers in the signal paths (note that the threshold voltage is simultaneously inverted), and  $V_C$  decreases until the negative threshold is reached. A reference signal propor-

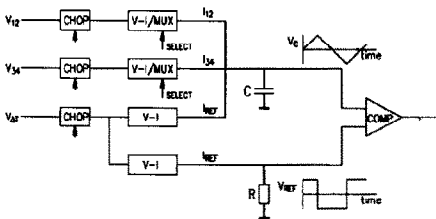


Fig 23 Frequency converter for a thermal flow sensor based on temperature-difference measurement

tional to the temperature difference  $\Delta T$  between sensor and flow is used, both to establish the threshold limits and the central frequency at zero flow. As a result the central frequency is determined only by the values of  $R$  and  $C$  ( $f_c = 1/4RC$ ), and can be measured periodically to include temperature and drift effects, by switching off both measurement channels. When selecting sequentially either of the two direction-signal channels, a frequency variation results which is proportional to the ratio of the flow-induced temperature differences and  $\Delta T$ .

#### Signal conversion in an intermediate domain

Signal conversion can be achieved more directly by using a transduction principle that naturally delivers a signal of the desired type. Examples of sensors with frequency output are the resonator sensors, like those where the (flow-dependent) temperature of the sensor is detected as a shift in resonance frequency of the structure, due to a change in thermal stresses [50, 51]. Also, the cooling of a thermal sensor heated by pulses can be used to obtain a duty-cycle or frequency signal [59, 60]. A specific implementation, where a direct digital conversion is obtained, is the so-called thermal sigma-delta modulator [61].

#### Signal conversion in the flow domain

Finally, the use of special flow-sensing techniques that inherently result in a time delay or a frequency may be appealing for the development of smart flow sensors. An example of the former is the time-of-flight technique [62, 63], where a small pulse of heat is released in the flow and the time it takes to travel the (fixed) distance between the heat source and a temperature detector downstream of it is measured. Alternatively, the heat source can be driven by an alternating current, and the time of flight is then determined as a shift in phase between the heater and temperature detector signals. Also, the time delay can be employed to control the frequency of a thermal resonator loop [64]. Inherent frequency-output signals are obtained when a measurement principle is used where an oscillating flow pattern occurs with a flow-dependent frequency [65], like the vortex shedding in the wake of a non-streamlined body [66]. In that case the shedding frequency increases proportionally to the flow velocity, and can be

detected by placing a thermal detector behind the vortex-generating body, or in a flow channel inside it. In the so-called fluidic feedback oscillator a specially shaped flow chamber is used, in which the flow changes periodically between two different flow patterns, again with a frequency proportional to the flow velocity [67].

## 9. Conclusions

We have discussed how thermal measurement principles can be used to realize integrated flow sensors. In the design and application of these sensors various aspects of the signal-transduction process were recognized, having a mechanical (flow), thermal (sensor transduction) and electrical (signal conditioning) nature, respectively. These were discussed in more detail in relation to the research that has been conducted in our laboratory on the development of direction-sensitive thermal-flow sensors and their application in an electronic wind meter without moving parts. Silicon etching can be used to improve the (thermal) performance of the sensors considerably. The extent to which these benefits can be exploited, however, and the sensor performance in general, depends strongly on the packaging and assembly of the sensor, which form an essential part of the sensor design. Some remarks were made on the perspectives of smart silicon flow sensors, using on-chip signal conversion in the electrical, thermal or even in the mechanical domain.

## Acknowledgements

The integrated flow sensor project of the Electronic Instrumentation Laboratory was started in 1975 and has been supervised by Professor J. H. Huijsing. During these years, many students and other colleagues have contributed to the project. Dr A. W. van Herwaarden is especially acknowledged for his contribution, in particular on the subject of the floating membrane sensor. All integrated sensors were manufactured at the IC Laboratory of the Department (presently incorporated in the Delft Institute for Microelectronics and Submicron Technology). The wind meter

prototype was made at the Mechanical Workshop of the Department. Flow experiments were carried out at the Low Speed Wind Tunnel Laboratory of the University. The project was supported by the Netherlands Foundation of Technology STW.

## References

- 1 P. Bradshaw, Thermal methods of flow measurement, *J Phys E Sci Instrum*, 1 (1968) 504–509
- 2 S. Middelhoek and S. A. Audet, *Silicon Sensors*, Academic Press, London, 1989
- 3 L. N. Krause and G. C. Fraulick, Miniature drag force anemometer, *NACA Technical Memorandum X-3507*, 1977
- 4 J. T. Sumito, G. J. Yeh, T. M. Spear and W. H. Ko, Silicon diaphragm capacitive sensor for pressure, flow, acceleration and attitude measurements, *Proc 4th Int Conf Solid-State Sensors and Actuators (Transducers 87)*, Tokyo, Japan, June 2–5 1987, pp 336–339
- 5 M. A. Schmidt, R. T. Howe, S. D. Senturia and J. H. Haritonidis, Design and calibration of a microfabricated floating-element shear-stress sensor, *IEEE Trans Electron Devices*, ED-35 (1988) 750–757
- 6 R. E. Hetrick, Vibrating cantilever mass flow sensor, *Sensors and Actuators A21–A23* (1990) 373–376
- 7 B. W. van Oudheusden, Silicon flow sensors, *IEE Proc D*, 135 (1988) 373–380
- 8 H. Schlichting, *Boundary Layer Theory*, McGraw-Hill, New York, 7th edn., 1979, pp 265–326
- 9 G. Comte-Bellot, Hot-wire and hot-film anemometers, in B. E. Richards (ed.) *Measurement of Unsteady Fluid Dynamic Phenomena*, Hemisphere Publishing Corporation, Washington, DC, 1977, pp 123–162
- 10 J. D. Vagt, Hot-wire probes in low speed flow, *Prog Aerosp Sci*, 18 (1979) 271–323
- 11 W. J. McCroskey and E. J. Durbin, Flow angle and shear stress measurements using heated films and wires, *J Basic Eng*, ASME Trans Series D, 94 (1972) 46–52
- 12 D. T. Gjessing, T. Lanes and A. Tangerud, A hot wire anemometer for the measurement of the three orthogonal components of wind velocity, and also directly the wind direction, employing no moving parts, *J Phys E Sci Instrum*, 2 (1969) 51–54
- 13 J. G. Olim, Split-film anemometer sensors, *Instrum Control Syst*, 43 (6) (1970) 106–108
- 14 D. S. Mahler, Bidirectional hot-wire anemometer, *Rev Sci Instrum*, 53 (1982) 1465–1466
- 15 B. E. Thompson and J. H. Whitelaw, Flying hot-wire anemometry, *Exp Fluids* 2 (1984) 47–55
- 16 R. A. Rasmussen, Application of thermistors to measurements in moving fluids, *Rev Sci Instrum*, 33 (1962) 38–42
- 17 A. Catellani, R. Stacchetti, A. Taromi and C. Canali, Performance and temperature stability of an air mass flowmeter based on a self-heated thermistor, *Sensors and Actuators*, 3 (1982/83) 23–30
- 18 K. Dostert, Applications of self-heated PTC-thermistors to flow and quantity of heat measurements, *Sensors and Actuators*, 3 (1982/83) 159–167
- 19 R. K. Steedman, A solid state oceanographic current meter, *J Phys E Sci Instrum*, 5 (1972) 1157–1162

- 20 L E MacHattie, The transistor as an anemometer, *J Phys E Sci Instrum*, 12 (1979) 754-760
- 21 W S Kuklinski, G Sadasiv and D Jaron, Integrated-circuit bipolar transistor array for fluid-velocity measurements, *Med Biol Eng Comput*, 19 (1981) 662-664
- 22 G E Platzer, Jr, Solid state fluid flow sensor, *US Patent No 3 992 940* (1976)
- 23 Tong Qin-Yi and Huang Jin-Biao, A novel CMOS flow sensor with constant chip temperature (CCT) operation, *Sensors and Actuators*, 12 (1987) 9-21
- 24 N Takata, A Jinda, J Takata, Y Inami and M Hijikigawa, Micro-chip flow sensors for measurement of flow velocity and direction, *Proc 4th Int Conf Solid-State Sensors and Actuators (Transducers '87)*, Tokyo, Japan, June 2-5, 1987, pp 352-335
- 25 A F P van Putten and S Middelhoek, Integrated silicon anemometer, *Electron Lett* 10 (1974) 425-426
- 26 J H Huijsing, J P Schuddemat and W Verhoef, Monolithic integrated direction-sensitive flow sensor, *IEEE Trans Electron Devices*, ED-29 (1982) 133-136
- 27 M Sekimura and S Shirouzu, Si flow sensor for velocity and direction sensing, *Proc 4th Sensor Symp, Japan*, 1984, pp 57-60
- 28 B W van Oudheusden and J H Huijsing, Integrated flow friction sensor, *Proc 4th Int Conf Solid-State Sensors and Actuators (Transducers '87)*, Tokyo, Japan, June 2-5, 1987, pp 368-371
- 29 B W van Oudheusden and J H Huijsing, Integrated silicon flow direction sensor, *Sensors and Actuators*, 16 (1989) 109-119
- 30 H Rahnamai and J N Zemel, Pyroelectric anemometers preparation and velocity measurements, *Sensors and Actuators*, 2 (1981) 3-16
- 31 D L Polla, R S Muller and R M White, Integrated multisensor chip, *IEEE Electron Device Lett*, 7 (1986) 254-256
- 32 B W van Oudheusden, Silicon thermal flow sensor with a two-dimensional direction sensitivity, *Meas Sci Technol*, 1 (1990) 565-575
- 33 B W van Oudheusden, The behaviour of a thermal-gradient sensor in laminar and turbulent shear flow, *J Phys E Sci Instrum*, 22 (1989) 490-498
- 34 A W van Herwaarden and P M Sarro, Thermal sensors based on the Seebeck effect, *Sensors and Actuators*, 10 (1986) 321-345
- 35 A W van Herwaarden, D C van Duyn, B W van Oudheusden and P M Sarro, Integrated thermopile sensors, *Sensors and Actuators*, A21-A23 (1990) 621-630
- 36 K E Petersen, Silicon as a mechanical material, *Proc IEEE*, 70 (1982) 420-456
- 37 O Tabata, Fast-response silicon flow sensor with an on-chip fluid temperature sensing element, *IEEE Trans Electron Devices*, ED-33 (1986) 361-365
- 38 O Tabata, H Inagaki and I Igarashi, Monolithic pressure-flow sensor, *IEEE Trans Electron Devices*, ED-34 (1987) 2456-2462
- 39 G N Stemme, A monolithic gas flow sensor with polyimide as thermal insulator, *IEEE Trans Electron Devices*, ED-33 (1986) 1470-1474
- 40 L Lofdahl, G Stemme and B Johansson, A sensor based on silicon technology for turbulence measurements, *J Phys E Sci Instrum*, 22 (1989) 391-393
- 41 M Stenberg, G Stemme, G Kittilsland and K Pedersen, A silicon sensor for measurement of liquid flow and thickness of fouling biofilms, *Sensors and Actuators*, 13 (1988) 203-221
- 42 Y C Tai and R S Muller, Lightly-doped polysilicon bridge as a flow meter, *Sensors and Actuators*, 15 (1988) 63-75
- 43 M Parameswaran, A M Robinson, Lj Ristic, K Chau and W Allegretto, A CMOS thermally isolated gas flow sensor, *Sensors Mater*, 2 (1990) 17-26
- 44 E Yoon and K D Wise, A dielectrically-supported multi-element mass flow sensor, *IEEE IEDM Tech Digest*, 1988, pp 670-673
- 45 B W van Oudheusden and A W van Herwaarden, High-sensitivity 2-D flow sensor with an etched thermal isolation structure, *Sensors and Actuators*, A21-A23 (1990) 425-430
- 46 D Moser, R Lenggenhager and H Baltes, Silicon gas flow sensors using industrial CMOS and bipolar IC technology, *Sensors and Actuators A*, 25-27 (1991) 577-581
- 47 K Petersen, J Brown and W Renken, High-precision, high-performance mass-flow sensor with integrated laminar flow micro-channels, *Proc 3rd Int Conf Solid-State Sensors and Actuators (Transducers '85)*, Philadelphia, PA, U S A June 7-11, 1985, pp 361-363
- 48 R G Johnson and R E Higashi, A highly sensitive silicon chip microtransducer for air flow and differential pressure sensing applications, *Sensors and Actuators*, 11 (1987) 63-72
- 49 M Esashi, S Eoh, T Matsuo and S Choi, The fabrication of integrated mass flow controllers, *Proc 4th Int Conf Solid-State Sensors and Actuators (Transducers '87)*, Tokyo, Japan, June 2-5, 1987, pp 830-833
- 50 S Bouwstra, P Kemna and R Legtenberg, Thermally excited resonating membrane mass flow sensor, *Sensors and Actuators*, 20 (1989) 213-223
- 51 S Bouwstra, R Legtenberg, H A C Tilmans and M Elwenspoek, Resonating microbridge mass flow sensor, *Sensors and Actuators*, A21-A23 (1990) 332-335
- 52 B W van Oudheusden and J H Huijsing, Microelectronic wind meter, *Proc 4th WMO Technical Conf Instrumentation and Methods Observation*, Brussels, 1989, pp 141-146
- 53 R E Bicking, L E Frazee and J J Simonelic, Sensor packaging for high-volume applications, *Proc 3rd Int Conf Solid-State Sensors and Actuators (Transducers '85)*, Philadelphia, PA, U S A, June 7-11, 1985, pp 350-353
- 54 A Grisel, C Francis, E Verney and G Mondin, Packaging technologies for integrated electrochemical sensors, *Sensors and Actuators*, 17 (1989) 285-295
- 55 H H van den Vlekkert, B Kloeck, D Prongue, J Berthoud, B Hu, N F de Rooij, E Gilli and Ph de Crousaz, A pH-ISFET and an integrated pH-pressure sensor with back-side contacts, *Sensors and Actuators*, 14 (1988) 165-176
- 56 J H Huijsing, Signal conditioning on the sensor chip, *Sensors and Actuators*, 10 (1986) 219-237
- 57 J W Bosman, J M de Bruijn, F R Riedijk, B W van Oudheusden and J H Huijsing, Integrated smart two-dimensional thermal flow sensor with Seebeck-voltage to frequency conversion, *Sensors and Actuators A*, 31 (1992), in press
- 58 H J Verhoeven, F R Riedijk and J H Huijsing, A smart bipolar thermal flow sensor with frequency output, *Proc 6th Int Conf Solid-State and Actuators (Transducers '91)*, San Francisco, CA, USA, June 24-27, 1991, pp 334-337
- 59 G Stemme, A CMOS integrated silicon gas-flow sensor with pulse-modulated output, *Sensors and Actuators*, 14 (1988) 293-303
- 60 Y Pan, F R Riedijk and J H Huijsing, A new class of integrated thermal oscillators with duty-cycle output for application in thermal sensors, *Sensors and Actuators*, A21-23 (1990) 655-659
- 61 J K Zelisse, F R Riedijk and J H Huijsing, Thermal sigma-delta modulator for wind speed and direction measurement, *Abst, Proc Workshop on Microelectronic Sensors*, Sozopol, Bulgaria, May 7-9, 1991, p 98
- 62 P M Handford and P Bradshaw, The pulsed-wire anemometer, *Exp Fluids*, 7 (1989) 125-132

- 63 C Yang, M Kummel and H Soeberg, A transit-time flow meter for measuring millimeter per minute liquid flow *Rev Sci Instrum*, 59 (1988) 314–317
- 64 J Kielbasa, J Rysz, A Z Smolarski and B Stasicki, The oscillatory anemometer, *Proc DISA Conf Fluid Dynamics Measurement in Industrial and Medical Environments, Leicester, U K 1972*, pp 65–68
- 65 R S Medlock, The vortex flowmeter—its development and characteristics, *Austr J Instrum Control*, 32 (1976) 24–34
- 66 T Robertson and J G Burns, An instrument for the automatic control of speed in low-speed wind tunnels, *J Phys E Sci Instrum*, 5 (1972) 598–600
- 67 P H Wright, The Coanda meter—a fluidic digital gas flowmeter, *J Phys E Sci Instrum*, 13 (1980) 433–436